Chapter 12

Quaternary Faulting on the Bare Mountain Fault

By Larry W. Anderson[1] and Ralph E. Klinger[1]

Contents

[1]U.S. Bureau of Reclamation, Denver, Colo.

Abstract

Quaternary activity on the Bare Mountain Fault was investigated by detailed mapping of Pleistocene surficial deposits and detailed studies in trenches and test pits excavated at three sites along the fault trace. The combined data show that along most of this 20-km-long, east-dipping, down-to-the-east normal fault, the contact between bedrock (Paleozoic and Precambrian sedimentary rocks) and alluvium (primarily fan deposits) is sharp and relatively linear, in some sections faulted and in others depositional. Prominent scarps in Quaternary deposits, indicative of late Quaternary fault activity, are present at a few scattered localities.

One faulting event is recorded in the surficial deposits exposed in one trench, and at least two faulting events in the other two trenches. Available evidence indicates that the most recent event (at all three trench sites) occurred no later than about 16±1 ka, possibly much earlier. A penultimate faulting event recorded at two sites probably occurred several tens of thousands to several hundred thousand years earlier. Still-earlier faulting events may have disrupted Quaternary deposits at one trench site, but the evidence is equivocal. Average displacement per event is estimated at 1.0 to 1.5 m.

Trench data indicate that the recurrence interval for moderate to large surface-rupturing paleoearthquakes on the Bare Mountain Fault is long, probably at least tens of thousands of years. The most recent faulting event is interpreted to have affected most of the length of the fault simultaneously, rather than causing rupture only on some short segments. The late Quaternary slip rate is estimated at 0.01 mm/yr.

Introduction

The Bare Mountain Fault is a major east-dipping, down-to-the-east normal fault that forms the structural boundary between Bare Mountain, a prominent upland of exposed Paleozoic and Precambrian rocks, and Crater Flat, a basin to

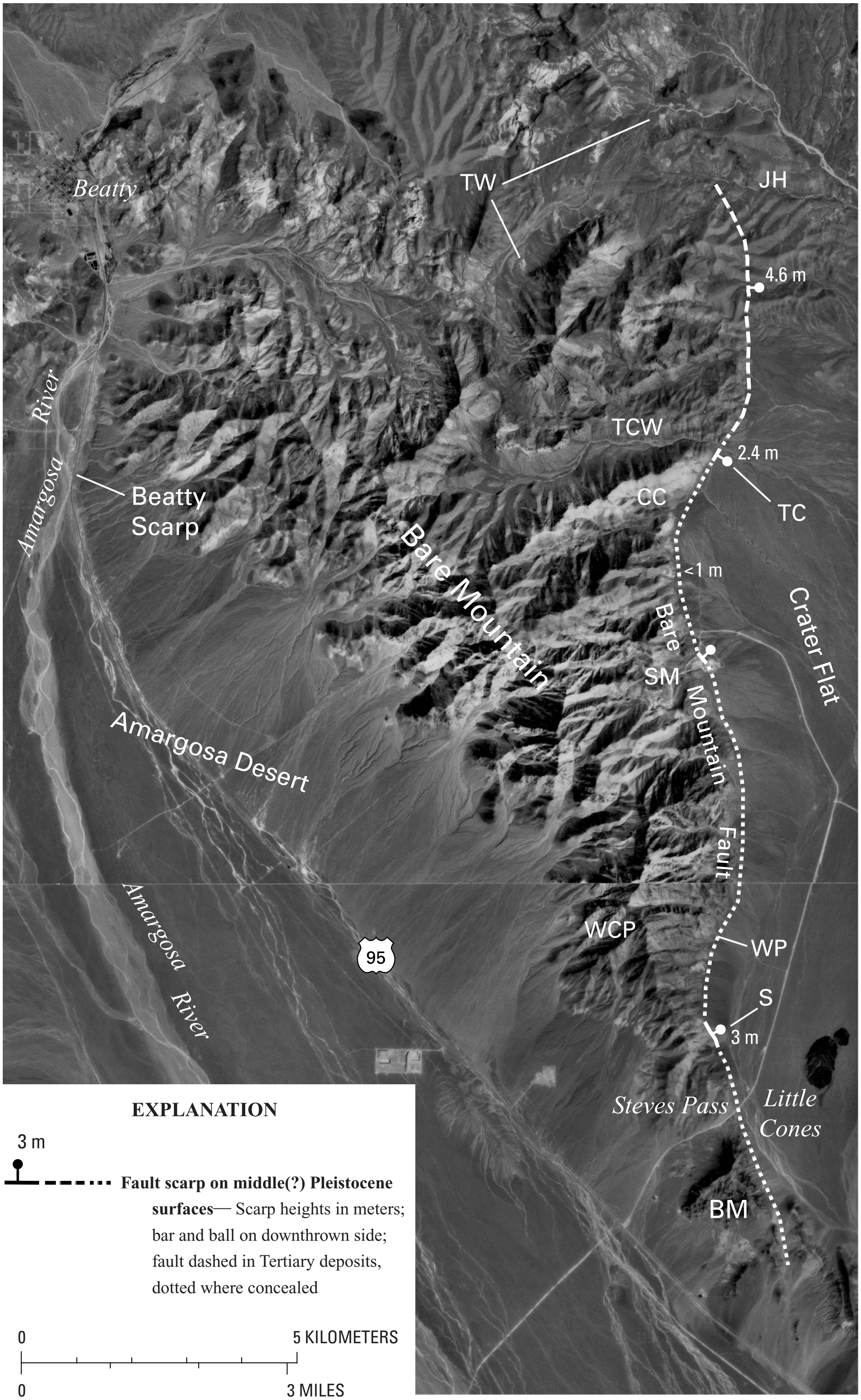

Figure 46. Bare Mountain Fault along east side of Bare Mountain, southwestern Nevada (figs. 1, 2). Trench sites: S, Stirling; TC, Tarantula Canyon; WP, Wildcat Peak. BM, Black Marble; CC, Chuckwalla Canyon; JH, Joshua Hollow; SM, Stirling Mine; TCW, Tarantula Canyon Wash; TW, Tates Wash; WCP, Wildcat Peak. Aerial-photographic mosaic from Project HAP–83, photographs 98–116 and 98–118, taken September 10, 1983.

the east that is filled by a thick sequence of Tertiary volcanic rocks and Quaternary alluvium (figs. 1, 46). Quaternary activity along the fault was first reported by Cornwall and Kleinhampl (1961), on the basis of (1) the sharp, relatively straight range front; (2) the small, relatively undissected alluvial fans along the east side of Bare Mountain; and (3) the linear alignment of Pleistocene volcanic cones in Crater Flat. A map by Swadley and Parrish (1988) showed that the range-front fault displaces lower Pleistocene deposits but is buried by younger, middle to upper Pleistocene deposits, whereas Reheis (1988) and Monson and others (1992) indicated that deposits as young as Holocene are faulted in several localities. Ferrill and others (1996) interpreted the slip rate on the Bare Mountain Fault to increase from north to south, partly because of an assumed change in the dip of the fault. During the present study, however, we determined on the basis of aerial-photographic interpretation and field mapping that (1) little evidence exists of latest Pleistocene or Holocene activity on the Bare Mountain Fault, (2) the dominant characteristic of most of the eastern range front of Bare Mountain is alluvium in depositional contact with bedrock, (3) actual displacements of Quaternary deposits are recognizable in only a few localities, and (4) the slip rate is low (~0.01 mm/yr) and does not increase (or change appreciably) from north to south.

The primary focus of this chapter is on the stratigraphic and structural relations of surficial deposits observed in natural exposures and trench excavations at three trench sites along the Bare Mountain Fault: Tarantula Canyon, Wildcat Peak, and Stirling (fig. 46).

Quaternary Stratigraphy

Surficial deposits, primarily alluvial fans of Quaternary age, were mapped earlier at a scale of 1:12,000 along the east flank of Bare Mountain by Anderson and Klinger (1996a). Colluvial and eolian deposits constitute much of the land surface in some areas, particularly near Black Marble (fig. 46), but they were not differentiated for this study. A common characteristic observed along the Bare Mountain range front is that older deposits have been eroded and are now covered with a thin (<1 m thick) veneer of younger material, as was also observed by Faulds and others (1994) and Peterson and others (1995) on the east side of Crater Flat near Yucca Mountain (fig. 1). Generally, we ignored this thin veneer in our mapping of surficial deposits during the present study.

We determined the relative ages of surficial deposits and associated geomorphic surfaces primarily by topographic position. We used the degree of desert-pavement development, the amount and degree of rock-varnish development on surface cobbles or boulders, the degree of preservation of original depositional topography (bar-and-swale topography), and, where observable, the degree of soil-profile development to distinguish and correlate the deposits. The criteria used for subdividing the surficial units along the east front of Bare Mountain are listed in table 35; these criteria are similar to those described by Hoover and others (1981), Swadley and others (1984), Taylor (1986), and Peterson and others (1995) for other surficial deposits at Yucca Mountain and in the adjacent areas. The geologic contacts are mostly similar to those of Swadley and Parrish (1988) and Monsen and others (1992), with only minor modifications; the few differences appear to result primarily from the larger scale of the mapping conducted for the present study.

Numerical ages of stratigraphic units were determined by Peterson and others (1995) at sites in Crater Flat. We examined surface characteristics and soil development at several of these sites to correlate the surficial deposits identified along Bare Mountain with dated deposits in nearby areas, as listed in table 36. The estimated ages of the Bare Mountain map units, based on regional stratigraphic correlations, are supported by the numerical ages of some of the deposits sampled in trenches along the range front during the present study. Neither felsic tephra erupted from regional sources (Izett and others, 1988) nor late Pleistocene basaltic ash erupted from local sources (for example, Heisler and others, 1999) that would aid in correlation and age assessments was identified along the Bare Mountain range front. Therefore, we consider the estimated ages and proposed correlations for the Bare Mountain surficial deposits to be only approximate. The estimated ages of various subdivisions of the Quaternary section are listed in table 4 (see chap. 2). Seven major surficial deposits, ranging in age from Miocene to Holocene, that were delineated along the east side of Bare Mountain are described below, in ascending order.

Miocene to Pliocene(?) Gravel

Stratified gravel deposits are present on a series of dissected hills and ridges at the northeast end of Bare Mountain, north of Tarantula Canyon and south of Joshua Hollow (fig. 46). Swadley and Parrish (1988) mapped these poorly consolidated deposits, and Monsen and others (1992) named them the Gravel of Sober-up Gulch. The deposits, at least 180 m thick, contain locally derived clasts of Proterozoic and Paleozoic sedimentary rocks, as well as clasts of Tertiary volcanic rocks. In the study area, the gravel beds are nearly flat-lying. Numerical ages of 7.7–8.7 Ma on tephra layers within the gravel deposits indicate a late Miocene age for the lower part of these deposits (Monsen and others, 1992).

Pliocene(?) to Lower Pleistocene Deposits

Pliocene(?) to lower Pleistocene deposits (unit Qta, table 35) have been identified only along the Bare Mountain range front, typically in small isolated remnants (for example, fig. 47). The deposits either are associated with the Bare Mountain Fault or are exposed locally in deep arroyos near the heads of alluvial fans. Unit Qta consists of gravel completely cemented with silica and carbonate. The original surfaces of the deposits are

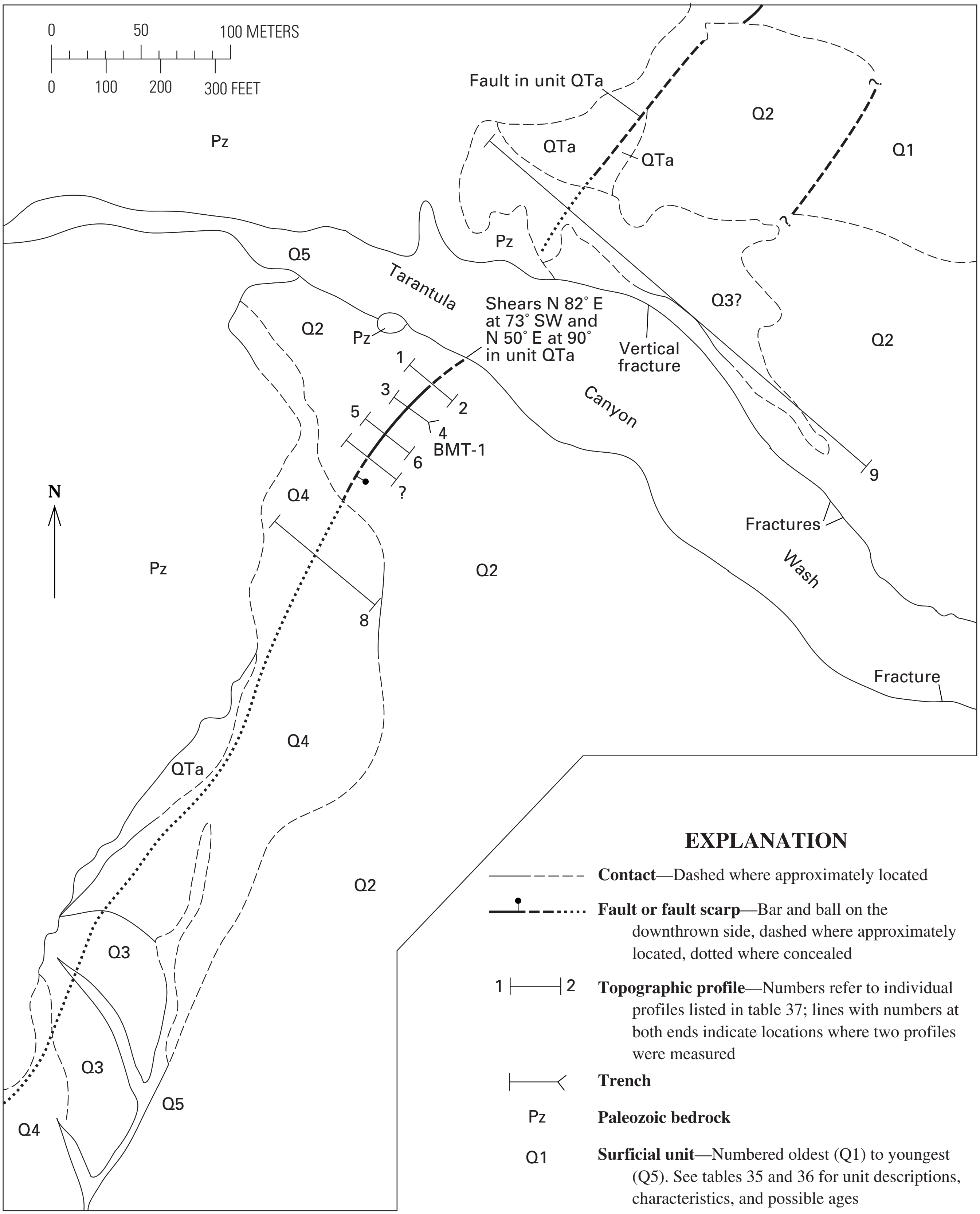

Figure 47. Geologic map of Tarantula Canyon trench site on the Bare Mountain Fault along east side of Bare Mountain, southwestern Nevada (pl. 20; figs. 1, 2). Base from enlarged low-Sun-angle aerial photograph taken in 1987 (State of Nevada, Yucca Mountain Low Sun Angle Project photograph 4–1a–10).

Table 35. Surface characteristics used to subdivide surficial deposits and geomorphic features along the Bare Mountain Fault, southwestern Nevada.

[See figures 1 and 2 for locations. Characteristics listed here may not depict the age of underlying deposits or reflect sedimentologic properties related to depositional history. Units are listed from youngest (top) to oldest (bottom). See table 3 for explanation of soil horizons]

Unit	Soil	Pavement	Desert varnish	Topography
Q5	May have weak Av/C profile; Av horizon <1 cm thick.	Generally absent; local incipient packing and horizontal orientation of clasts.	None	High-relief bar and swale.
Q4	Thin Av horizon (several centimeters thick).	Poorly packed	Weakly developed on quartzite clasts.	Bar and swale distinct but subdued; bars are coarser grained than adjacent swales.
Q3	Moderately well developed Av horizon (5–10 cm thick).	Moderately well to well packed on bars.	Moderately well developed on quartzite clasts.	Bar and swale subdued; transition between bars and swales diffuse.
Q2	Well-developed Av horizon (>10 cm thick).	Moderately well to well packed; carbonate rinds on clasts, fragments common in pavement.	Well developed on surface clasts.	Little or no evidence of bar and swale; surface is nearly smooth.
Q1	Av horizon may or may not be present, depending on topographic position.	Moderately well to well packed; pavement is being degraded; underlying petrocalcic horizon is locally exposed.	Moderately well to well developed on some surface clasts, absent on others.	Surface is dissected; small rills and drainages common.
QTa	Gravel completely cemented with carbonate or silica, or both; in places, surface veneered by younger unconsolidated deposits.	None	None	No original surfaces preserved.

Table 36. Correlation chart for Quaternary alluvial deposits in the vicinity of the Bare Mountain Fault, southwestern Nevada.

[See figures 1 and 2 for locations. Correlation is based on surface morphology and soil characteristics. Boundaries between the Holocene and Pleistocene and between the Pleistocene and Pliocene are dated at 10 and 1,650 ka, respectively]

Series	Bare Mountain			Crater Flat (Peterson and others, 1995)
	This study	Swadley and Parrish (1988)	Monsen and others (1992)	
Holocene	Q5	Q1a Q1b (<0.14 ka)	Qyf	Modern Crater Flat (>0.3–>1.3 ka)
	Q4	Q1c (<10 ka)		Little Cones (>6–>11 ka)
Pleistocene	Q3	Q2a	Qif	Late Black Cone (>17–>30 ka)
		Q2b (145–160 ka)		Early Black Cone (>159–>201 ka)
	Q2			
		Q2c (270–430 ka)		Yucca (>375 ka)
	Q1	?	QTof	Solitario (>433–659 but <730 ka)
Pliocene	QTa	Qta (1,100–2,000 ka)		

not preserved. The unit QTa deposits identified during the present study, which generally correspond to unit QTa of Swadley and Parrish (1988; see chap. 2; table 2), probably accumulated over a lengthy time interval. Although exposures are limited, no clasts of Tertiary volcanic rocks were observed in unit QTa deposits. Thus, the unit is apparently much younger than the Miocene to Pliocene(?) gravel described above.

Lower to Middle Pleistocene Deposits

Lower to middle Pleistocene deposits (unit Q1, table 35) are present at the surface primarily along the northern part of the Bare Mountain range front, north of the Sterling Mine (SM, fig. 46). The surfaces of these deposits are highly dissected, resulting in a ballena (rounded ridge and ravine) morphology, and are commonly littered with abundant carbonate rubble. Some quartzite clasts have a dark varnish. Av soil horizons may or may not be present. A test pit was excavated on a unit Q1(?) surface about 1.2 km south of Chuckwalla Canyon (CC, fig. 46). The soil profile is characterized by Av-Bk-Bw horizons to about 50-cm depth that overlie a strongly developed Bk horizon with $CaCO_3$ stage IV–V morphology (nomenclature of Birkeland, 1984). In most areas, however, the upper soil horizons have apparently been stripped, leaving the Bk horizon at or near the surface. On the basis of morphology and soil characteristics, unit Q1 is correlated with the Solitario or Yucca deposits of Peterson and others (1995), thus probably ranging in age from 375 to 730 ka (table 36).

Middle Pleistocene Deposits

Middle Pleistocene deposits (Q2, table 35) are common in the map area north of the Sterling Mine (SM, fig. 46). The large alluvial fan that emanates from Tarantula Canyon Wash (TCW, fig. 46) generally has the characteristics of a unit Q2 surface. Like most older deposits in the Bare Mountain area, the unit Q2 deposits probably span a long time interval and are dated at middle Pleistocene.

Surfaces on Q2 deposits are characterized by well-developed Av soil horizons (in some places >10 cm thick), moderately well packed to well-packed pavements, dark varnish on quartzite clasts, and a general absence of bar-and-swale topography. In many areas, however, especially adjacent to the range front, unit Q2 alluvial fans are typically buried by a thin veneer of younger unit Q4 deposits consisting of locally derived colluvial and eolian materials. Where this veneer is thin (<1 m thick), it does not seem to totally mask the better-developed surface characteristics of unit Q2 deposits. Soils characterized by A-Bw-Bk horizons that overlie strongly developed Bk horizons with $CaCO_3$ stage III–IV+ or silica morphology are also typical of these deposits in some localities. The surface characteristics and soil development indicate that unit Q2 approximately correlates with the Early Black Cone or Yucca deposits of Peterson and others (1995) and unit Q2c of Swadley and Parrish (1988) (table 36). Thus, unit Q2 is considered to range in age from 159 to 430 ka. Further constraints on the age of unit Q2 are discussed below in the subsection entitled “Stirling Trench Site.”

Upper Pleistocene Deposits

Upper Pleistocene deposits (unit Q3, table 35) are the least common of the Quaternary units along the east side of Bare Mountain, represented by small fan remnants adjacent to the range front, with surface characteristics intermediate between those of units Q2 and Q4. In several areas, unit Q3 surfaces were initially identified on aerial photography by their height above adjacent unit Q4 surfaces. Subsequent field mapping revealed that the surface characteristics of unit Q3 also are more strongly developed than those of unit Q4. Unit Q3 surfaces have moderately well developed Av soil horizons (5–10 cm thick), moderately well packed to well-packed pavements, moderately developed varnish on quartzite clasts, and subdued bar-and-swale topography.

Soil on a possible unit Q3 remnant, exposed in a pit near Wildcat Peak (WP, fig. 46), is characterized by Avk-Bk horizons over a Bkb horizon with $CaCO_3$ stage II–III morphology. On the basis of its topographic position, surface morphology, and soil-profile characteristics, unit Q3 is probably correlated with unit Q2a of Swadley and Parrish (1988) and the Late Black Cone deposits of Peterson and others (1995) (table 36). Like other deposits along the eastern Bare Mountain range front, unit Q3 may range in age from about 17 to 100–200 ka.

Upper Pleistocene to Holocene Deposits

Upper Pleistocene to Holocene deposits (unit Q4, table 35) are some of the most abundant surficial deposits adjacent to Bare Mountain. They are characterized by thin (<5 cm thick) Av soil horizons, poorly developed desert pavement, weakly developed rock varnish on quartzite clasts, and distinct bar-and-swale topography. Unit Q4 soils typically have only Av-Avk-Bk horizons, with only $CaCO_3$ stage I–II morphology. The deposits are thin (1–3 m thick), typically forming a thin veneer over older deposits. As exposed in a test pit near Steves Pass (fig. 1), for example, they are 1.25 m thick, overlying a much older (unit Q2?) deposit with $CaCO_3$ stage III+–IV morphology. Unit Q4 has been differentiated only where it is thick enough (generally >1 m) to completely mask the underlying deposits.

Unit Q4 correlates with unit Q1c of Swadley and Parish (1988) and the Little Cones deposits of Peterson and others (1995). Thus, unit Q4 could range in age from only a few thousand years to 20 ka.

Upper Holocene to Modern Deposits

Upper Holocene to modern deposits (unit Q5, table 35) consist of coarse gravelly sand deposited in or adjacent to active washes. The deposits are characterized by their unweathered appearance, pronounced bar-and-swale topography, general absence of soil development (generally weak Av over C horizons), and absence of vegetation, rock-varnish, and desert-pavement development. No soils were described on the unit Q5 deposits. Unit Q5 probably correlates with units Q1a and Q1b of Swadley and Parish (1988) and the late Crater Flat deposits of Peterson and others (1995) (table 36), indicating that they are only a few thousand years old at most.

Characteristics of the Bare Mountain Fault

Tates Wash to Tarantula Canyon Wash

The northernmost section of the Bare Mountain Fault is about 5 km long, extending from Joshua Hollow (JH, fig. 46) and Tates Wash (TW) on the north to Tarantula Canyon Wash (TCW) on the south. From Joshua Hollow southward for a distance of about 2 km, the fault is identifiable by tonal and vegetation lineaments primarily on Miocene and Pliocene(?) gravel and bedrock. The fault strikes N. 30° W. to nearly due north. Monsen and others (1992) showed alluvial-fan deposits of early Pleistocene and (or) Pliocene age to be faulted at Joshua Hollow Wash, but unequivocal evidence of faulting and a definitive scarp were not observed during the present study. At an unnamed wash about 2 km south of Joshua Hollow, the fault strikes nearly north-south, and a 4.6-m-high scarp is present on a small unit Q1 terrace. This scarp is the northernmost scarp that we identified along the fault zone. Between this unnamed wash and Tarantula Canyon, the fault consists of several strands that generally strike north. This section of the fault includes one scarp, 11 m high, on Miocene to Pliocene(?) gravel deposits.

At an unnamed wash 1.5 km north of Tarantula Canyon (TC, fig. 46), unit Q3 (table 35), overlies the Bare Mountain Fault without displacement. At a point about 0.5 km north of Tarantula Canyon, the fault strike changes to a more northeasterly trend. In this area, the fault is expressed as a fault contact between bedrock and unit QTa deposits and lower Quaternary deposits (units Q1, Q2). In several prospect pits, faults and shears in silica- and carbonate-cemented deposits (unit QTa) dip 45°–70° E. Small (less than 50 cm high) ridges of silica- and carbonate-cemented rock (unit QTa?), commonly with slickensides, are also present in several localities.

Tarantula Canyon Wash to Chuckwalla Canyon

The Bare Mountain Fault strikes about N. 50° E. from Tarantula Canyon Wash (TCW, fig. 46) on the north to Chuckwalla Canyon (CC) on the south. The most notable feature along this 2-km-long section of the fault is a fairly prominent, 1- to 2-m-high scarp on a middle Pleistocene alluvial fan (unit Q2, table 35) immediately south of Tarantula Canyon Wash that was identified by Swadley and Parrish (1988). The locality (Tarantula Canyon trench site, fig. 47) was selected for detailed study, as discussed below.

Reheis (1988) and Monsen and others (1992) showed that young alluvial-fan deposits are displaced along most sections of the Bare Mountain Fault between Tarantula Canyon Wash and Chuckwalla Canyon. However, no scarps on units Q3 and Q4 (table 35) alluvial-fan deposits were identified during the present study. Much of the fault is expressed as a fault contact between bedrock and unit QTa and as faults and shears that dip 30°–70° SE. in silica- and carbonate-cemented deposits (unit QTa) exposed in several prospect pits near Chuckwalla Canyon.

Chuckwalla Canyon to South of Wildcat Peak

The central section of the Bare Mountain Fault extends for approximately 10 km, from Chuckwalla Canyon (CC, fig. 46) on the north to just south of Wildcat Peak (WP). The fault strikes generally north and is marked for much of its length by an abrupt, fairly linear bedrock-alluvium contact. A scarp, which was identified by Swadley and Parish (1988), is present on unit Q1 (table 35) deposits near the Sterling Mine (SM, fig. 46). In a few places, evidence for Quaternary faulting involves exposures of unit Qta or Q1 deposits at or west of the range front. If the surface elevations of these deposits were extended eastward, they would project above the levels of surfaces on younger deposits (Swadley and Parrish, 1988), thus indicating fault offset. Evidence of Quaternary faulting is also indicated by sheared silica- and carbonate-cemented gravel (unit Qta?) exposed in several prospect pits (Reheis, 1988). Aerial photographs show a lineament on a unit Q3 alluvial fan 0.5 km north of the Sterling Mine. On the ground, the lineament appears to be an older scarp on a unit Q1 deposit that is nearly buried by a veneer of unit Q3 deposits. Relief across the feature is less than 1 m.

Immediately south of the Sterling Mine (SM, fig. 46), a silica- and carbonate-cemented shear is present in a unit Q2 (table 35) alluvial fan. Reheis (1988) identified similar shears in two trenches along the fault; exposures in one trench (BMT–2, fig. 48), immediately east of Wildcat Peak, led Reheis (1988) to conclude that the Bare Mountain Fault in this area had been the locus of late Pleistocene and, possibly, Holocene activity. Our mapping, however, indicates that unit Q3 alluvial fans apparently overlie the fault in several localities, indicating that the most recent fault activity in this area may be older than that reported by Reheis (1988). Primarily on the basis of the conclusions of Reheis (1988), the Wildcat Peak trench site (WP, fig. 46) was selected for additional study, as discussed below.

South of Wildcat Peak to Black Marble

The southern section of the Bare Mountain Fault extends for about 3 km, from just south of Wildcat Peak (WP, fig. 46) to the south end of Black Marble (BM). Near Wildcat Peak, the fault strikes due north, but at a point about 1 km southeast of

Wildcat Peak it changes in strike to approximately N. 30° W. At this point (Stirling trench site, fig. 49), a 1- to 3-m-high scarp trends north to northwest across a unit Q2 alluvial fan. This scarp, which was recognized by Monsen and others (1992), is the southernmost fault scarp identified during the present study. Owing to the presence of this scarp, the Stirling trench site was identified for detailed study, as discussed below. From the south end of the Stirling site to the south end of Black Marble, the Bare Mountain Fault is concealed by upper Pleistocene to Holocene alluvial fans (units Q3, Q4, table 35).

South of Black Marble

Bare Mountain loses its steep, linear, range-front morphology south of Black Marble (BM, fig. 46). The mountain also decreases in relief, basically terminating at the south end of Black Marble, but Paleozoic bedrock forms a series of low north-northwest-trending hills for a distance of about 3 km south of Black Marble. East-dipping Tertiary volcanic rocks (Miocene Timber Mountain Group) that are exposed farther to the southeast are topographically higher than the Paleozoic rocks; the

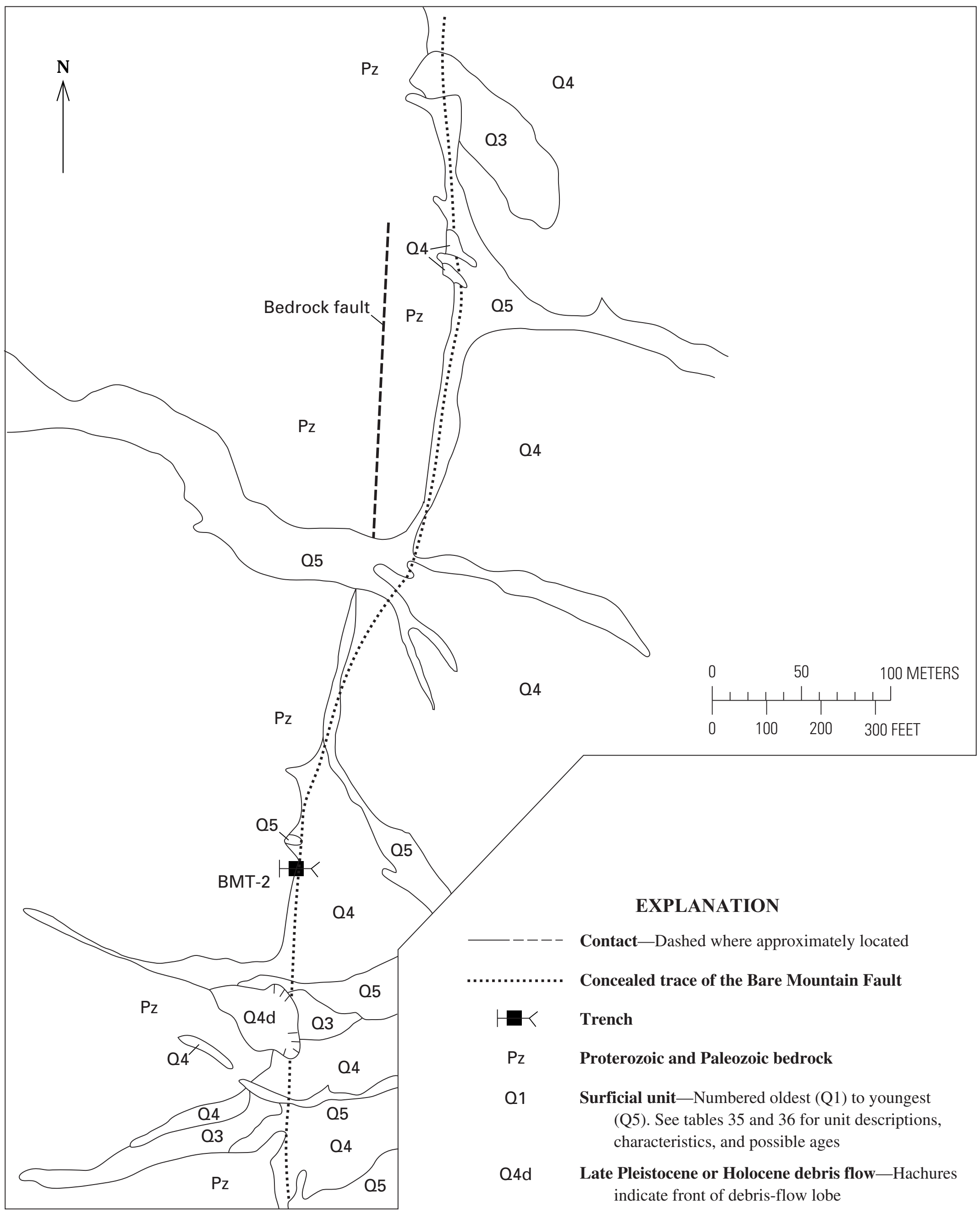

Figure 48. Geologic map of Wildcat Peak trench site on the Bare Mountain Fault along east side of Bare Mountain, southwestern Nevada (pl. 21; figs. 1, 2). Base from enlarged low-Sun-angle aerial photograph taken in 1987 (State of Nevada, Yucca Mountain Low Sun Angle Project photograph 4–1a–4).

volcanic rocks form the south margin of Crater Flat. No evidence of late Quaternary displacement was observed in this area.

Small outcrops of tilted and faulted Tertiary sedimentary rocks are present south of Black Marble (Swadley and Carr, 1987), indicating that post-Miocene faulting has occurred along the projection of the Bare Mountain Fault southeast of Black Marble. Geologic and geomorphic evidence obtained during the present study, however, indicates that little, if any, movement occurred on the Bare Mountain Fault in the area south of Black Marble during the late Quaternary.

Detailed Study Sites

Three trench sites—Tarantula Canyon, Wildcat Peak, and Stirling (figs. 47, 48, and 49, respectively)—were identified for detailed study of the Bare Mountain Fault. Two of the trench sites (Tarantula Canyon and Stirling) are located where distinct scarps are present on what appear to be middle Pleistocene (unit Q2, table 35) alluvial fans. Detailed study at these two sites consisted of geologic mapping, topographic

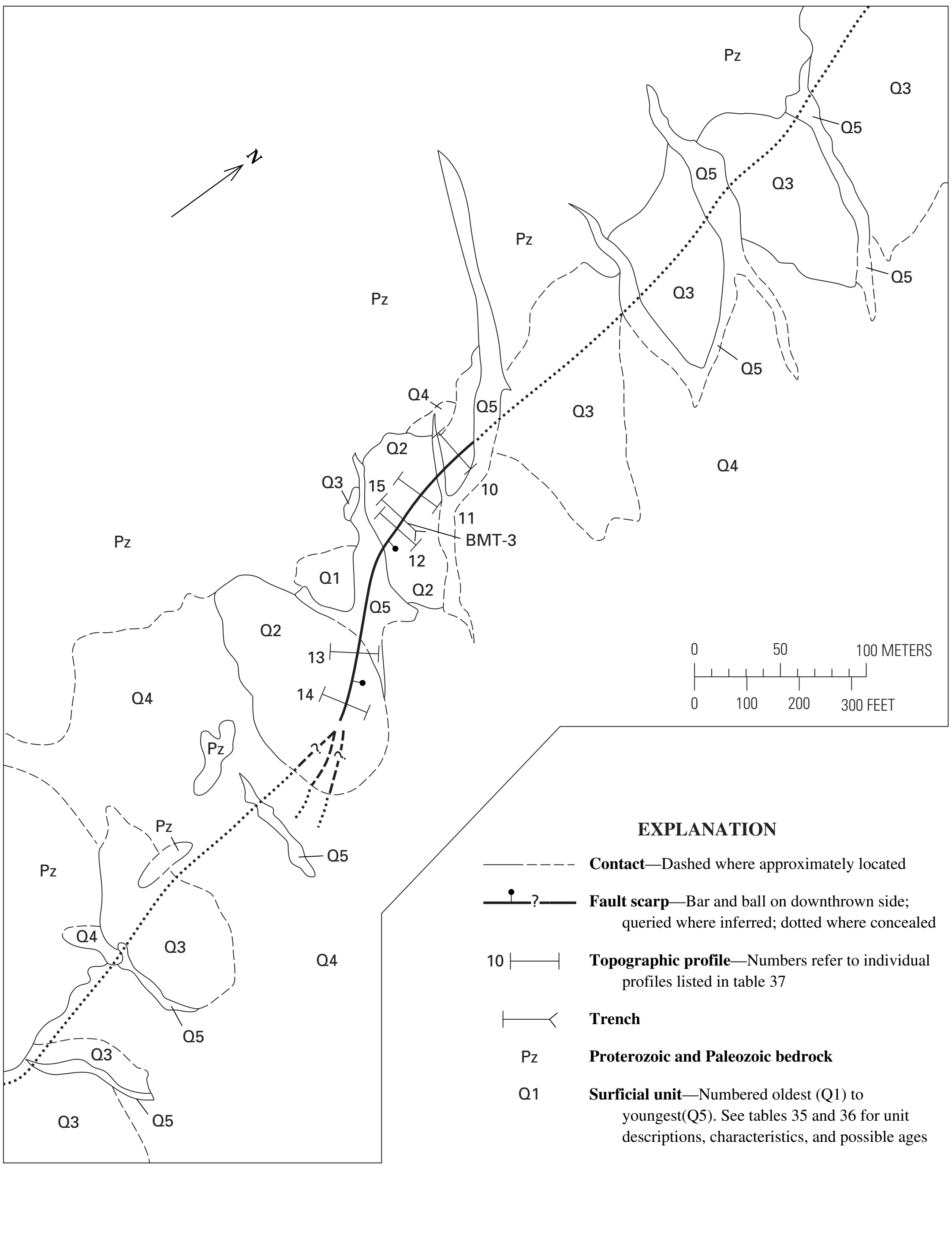

Figure 49. Geologic map of Stirling trench site on the Bare Mountain Fault along east side of Bare Mountain, southwestern Nevada (pl. 22; figs. 1, 2). Base from enlarged low-Sun-angle aerial photograph taken in 1987 (State of Nevada, Yucca Mountain Low Sun Angle Project photograph 4–1a–3).

profiling of the scarps, excavation of trenches across the scarps, mapping of the trench exposures, description of the soils and deposits exposed in the trenches, and collection of samples for numerical dating. The third trench site (Wildcat Peak) originally was a prospect or mineral-exploration pit; geologic relations exposed in the pit were initially described by Reheis (1988). Although a topographic scarp on alluvium is absent at this site, detailed mapping was conducted, and the former prospect pit was enlarged. The new excavation was also mapped in detail, soils were described, and samples were collected for numerical dating. In the following sections, we discuss the results of detailed study at these three trench sites.

Tarantula Canyon Trench Site

The Tarantula Canyon trench site (pl. 20), immediately east of the mouth of Tarantula Canyon (TC, figs. 46, 47) on the south side of the wash, is the only locality along the Bare Mountain range front where a fault scarp is present on a relatively flat alluvial fan.

The scarp, just south of the wash, is about 110 m long and as much as 2.4 m high. The surface on which the scarp is preserved was mapped as a unit Q2 alluvial fan (fig. 47; table 35), although its surface characteristics are not as well developed as on most unit Q2 surfaces in the study area. In the immediate vicinity of the scarp and adjacent to the range front, the unit Q2 alluvial fan is buried by a thin (<50 cm thick) veneer of younger alluvial, colluvial, and eolian deposits (not shown in fig. 47). This veneer, which is probably equivalent to unit Q4 deposits, is no older than early Holocene on the basis of the presence of artifacts dated at about 7 ka (G.M. Haynes, written commun., 1995).

North of Tarantula Canyon Wash (TCW, fig. 46), the Bare Mountain Fault is buried by younger unit Q2 or older unit Q3 deposits (mapped as unit Q3? in fig. 47) that appear to have originated as a debris flow from a small drainage north of Tarantula Canyon. The morphology and stratigraphic relations of these deposits indicate that they predate the incision of Tarantula Canyon Wash. The soil on this debris-flow deposit is well developed, with a B (Bt) horizon that has a sandy-clay texture, strong blocky structure, distinct clay films on ped faces and in pores, and a carbonate horizon with $CaCO_3$ stage II+ morphology. These characteristics support an age of at least late Pleistocene for the debris flow.

Farther north, the main fault trace is marked by scattered outcrops of silica- and carbonate-cemented gravel (unit QTa, table 35), in some places with linear fault-scarp-like ridges, 30 to 40 cm high. Faults and shears that strike N. 30°–40° E. and dip 47°–90° E. are exposed in two test pits north of Tarantula Canyon Wash (TCW, fig. 46). Scarps on younger Quaternary fans are absent to the north, primarily because no extensive late Pleistocene deposits are present in that area. Several silica- and carbonate-cemented fractures are observable in the walls of the wash downstream from the mouth of the canyon, and faint tonal, topographic, and vegetation lineaments are present on adjacent fan surfaces above the carbonate-cemented fractures. No displacements of distinct gravel beds were observed across any of these fractures; thus, a faulting (as opposed to fracturing) origin for these features is questionable.

About 200 m south of Tarantula Canyon Wash (TCW, fig. 46), the fault trace is marked by unit QTa outcrops. Although Monsen and others (1992) indicated that Holocene alluvial fans are faulted along this section of the fault, we observed no evidence of Holocene faulting. The fault is clearly buried by unit Q3 (late Pleistocene) and unit Q4 (latest Pleistocene to middle Holocene) deposits along this section (fig. 47).

Topographic Profiles

Nine topographic profiles were measured near the mouth of Tarantula Canyon (TC, figs. 46, 47). Topographic profiling has been widely used in the Western United States to approximate the ages of fault scarps (Wallace, 1977, 1980; Bucknam and Anderson, 1979; Nash, 1980, 1984; Machette and others, 1984; Hanks and Andrews, 1989). The technique is based on the assumption that a scarp developed in unconsolidated materials (regardless of origin) will degrade in a relatively predictable manner. Nash (1986) provided a good review of this technique.

On the south side of the Tarantula Canyon Wash (TCW, fig. 46), seven profiles (1–7, fig. 47) were measured across the scarp on the unit Q2 (table 35) surface. Farther south, one profile (8) was measured on a unit Q4 surface across a photolineament that trends southwest along the projected trend of the scarp on the unit Q2 surface. One 220-m-long profile (9) was measured on the north side of the wash, across the projection of the fault and scarp from the south side of the wash. Three profiles (1, 3, 5) were measured manually by using a tape, stadia rod, and hand level; the other six profiles (2, 4, 6–9) were measured by using an electronic surveying instrument (total station). An average of 7 measurements were made per profile to construct profiles 1, 3, and 5 (56–84 m long), and an average of 25 measurements per profile for profiles 2, 4, 6, and 7 (69–85 m long). The scarp heights, surface offsets, and maximum scarp-slope angles, which were measured from computer-generated plots of the profiles, are listed in table 37. The scarp heights of profiles measured on the unit Q2 surface (profiles 1–7) range from 1.1 to 2.4 m, surface offsets from 0.4 to 1.9 m, and maximum scarp-slope angles from 5.5° to 10°. The absence of compound scarps or obvious bevels in the profiles indicates that the Tarantula Canyon scarp resulted from a single faulting event. No scarp is discernible in the profiles measured across the photolineament south of Tarantula Canyon or across the projection of the fault scarp north of the wash in profiles 8 and 9, respectively, both of which were measured on surfaces younger than the unit Q2 alluvial fan containing the scarp.

In figure 50, maximum scarp angles are plotted against scarp heights for profiles across the scarp at Tarantula Canyon (TC, figs. 46, 47), along with plots for profiles measured across the Beatty scarp on the west side of Bare Mountain (Anderson and Klinger, 1996b). The age of the Beatty scarp is relatively well constrained by radiocarbon ages of about 9–13 ka (Swadley and others, 1988; Anderson and Klinger, 1996b). Superimposed on the scarp-profile data are a series of regressions calculated by Bucknam and Anderson (1979) for scarps of known age in the Great Basin Province. Data derived from the three profiles measured manually (1, 3, 5) cluster together and plot lower in figure 50 than those from the profiles measured electronically with the total station, even though profiles 1, 3, and 5 were measured along basically the same transects as profiles 2, 4, and 6, respectively. (Bucknam and Anderson's profiles were measured manually.) We conclude that the data collected manually, owing to the fewer number of points and the greater distance between measurements, yield profiles that are artificially smoothed and have lower scarp angles than do the profiles measured with surveying instruments. Regardless of slight differences in the data, the Tarantula Canyon scarp is clearly much older than the Beatty scarp because of the much lower maximum scarp-slope angles for the Tarantula Canyon scarp (fig. 50), which may be as old as 100 ka, on the basis of comparisons with the Beatty scarp.

Table 37. Data from topographic profiles on fault scarps along the Bare Mountain Fault, southwestern Nevada.

[All values were measured by hand and from computer-generated plots of profiles. Profiles 1–9 were measured at the Tarantula Canyon trench site (fig. 47), and profiles 10–15 at the Stirling trench site (fig. 49). Profiles 1, 3, and 5 were measured with hand level and stadia rod, profile 15 with hand level and 0.5-m-long rod, and all other profiles with electronic surveying instrument (total station). No scarp was observable in profiles 8 and 9. Profile 3 was measured along axis of trench BMT–1 (pl. 20) before excavation, and profile 4 immediately south of trench]

Profile	Scarp height (m)	Surface offset (m)	Maximum scarp-slope angle (°)	Surface-slope angle (°)
1	2.0	1.6	5.5	1.0
2	1.4	.9	7.0	2.0
3	2.2	1.5	6.0	1.5
4	2.4	1.9	10.0	1.5
5	1.9	1.5	6.0	1.0
6	1.8	1.1	8.5	2.0
7	1.1	.4	7.5	3.0
8	– –	– –	– –	– –
9	– –	– –	– –	– –
10	1.2	.8	14.0	5.0
11	2.5	1.1	18.0	9.5
12	2.3	1.1	17.5	8.5
13	1.3	.5	18.0	8.5
14	2.7	.9	15.0	8.5
15	3.3	.8	20.0	11.0

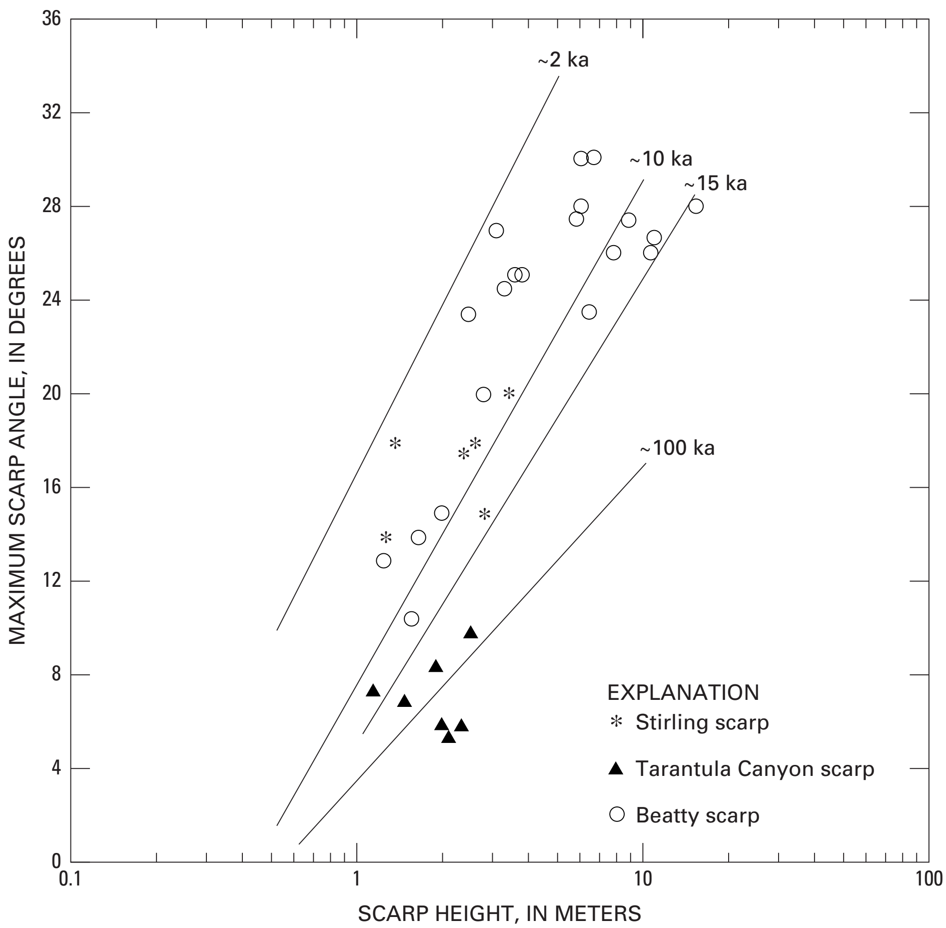

Figure 50. Scarp height versus maximum scarp-slope angle for topographic profiles of Stirling and Tarantula Canyon scarps along the Bare Mountain Fault on east side of Bare Mountain, southwestern Nevada (figs. 1, 2), in comparison with those of the Beatty scarp (Anderson and Klinger, 1996b) and regression lines for scarps of known age in the Basin and Range Province (modified from Bucknam and Anderson, 1979).

Stratigraphy

Trench BMT–1 (pl. 20; figs. 1, 47) is a 43-m-long excavation across the Bare Mountain Fault scarp at Tarantula Canyon (TC, figs. 46, 47). The oldest unit (I) recognized in the trench is known to be present only on the south wall (stas. 18–20 m, pl. 20); the upper part of this unit may also be present but was not identified with certainty in the floor of the trench (sta. 11 m). This indurated gravelly sand, which appears to be primarily of fluvial origin, is probably equivalent to unit QTa of Swadley and Parrish (1988), on the basis of its degree of induration and its relation to overlying deposits. Unit QTa is at the surface both north and south of the trench site (fig. 47). The contact between units I and II is sharp and distinct and appears to be an unconformity (pl. 20).

Unit II (pl. 20) is a moderately well stratified to well-stratified sandy gravel. A well-developed calcic horizon ($CaCO_3$ stage IV–IV+ morphology), 0.7 to 1.5 m thick, is present in the upper part of the unit. Unit III, consisting of gravelly-silty clay, is preserved only in the eastern part of the trench. The unit is interpreted to be an argillic (Bt) soil horizon associated with the calcic soil horizon formed in unit II. Whereas unit II is a fluvial gravel deposited by the main Tarantula Canyon stream, unit III consists of finer grained colluvium, fluvial, and eolian material that accumulated after abandonment and stabilization of the fan surface. Though differing from each other both genetically and texturally, the soil horizons developed on units II and III are believed to be part of the same soil because of their interrelations and the continuity of their boundaries. The relations between units II and III also indicate that their ages are similar.

Units II and III (pl. 20) are correlated with unit Q2 (table 35) on the basis of soil similarities. The strong development of the pedogenic carbonate ($CaCO_3$ stage IV–IV+ morphology), both in the upper part of unit II and in the test pit, indicates some antiquity for these deposits (Birkeland and others, 1991; Bull, 1991). These relations also indicate that unit Q2 probably correlates with unit Q2c of Swadley and others (1984) and Swadley and Parrish (1988) and with the Early Black Cone or Yucca unit of Peterson and others (1995) (table 32); thus, the minimum age of units II and III is estimated at 159 ka.

The uppermost and youngest unit (IV) in the trench consists of massive gravelly silt, considered to be correlative with unit Q4 (table 35) that forms only a thin veneer at the trench site and was not mapped at the surface (fig. 47). An archeological survey of the trench site before excavation recovered artifacts dated at least 7 ka from this unit (G.M. Haynes, written commun., 1995). A sample (TL–31, pl. 20; table 38) from unit IV collected for thermoluminescence analysis yielded an age of 6±1 ka, which is consistent with the estimated age of the artifacts and considered to be a minimum age for the unit (latest Pleistocene to early Holocene).

A weakly developed carbonate cement ($CaCO_3$ stage I+ morphology) in trench unit III (for example, stas. 17–18 m, pl. 20), is believed to be of late Pleistocene age. A sample (TL–32, pl. 20; table 38) from unit III yielded an age of 16±1 ka, which may represent the time when unit III was buried by unit IV. This age also provides a minimum date for the carbonate overprinting on unit III because carbonate probably began to accumulate shortly after the burial of unit III by unit IV. Such a date agrees with Peterson and others' (1995) age (>17–>30 ka) for the soil development on the Late Black Cone deposits (table 36). Thermoluminescence ages of buried soil horizons generally represent minimum dates for burial of the horizon (Forman and others, 1988). In the setting described above, however, the thermoluminescence age may reflect the latest infiltration and accumulation of carbonate with $CaCO_3$ stage I+ morphology, thus providing a minimum date for the latest faulting event.

Interpretation of Quaternary Fault Activity

A conspicuous fault, dipping 72° E. and coincident with the base of the surface scarp, is exposed on the south wall of trench BMT–1 (stas. 18–19 m, pl. 20; figs. 1, 47). The fault clearly displaces units I and II and part of unit III, apparently during a single faulting event. Although unit IV thickens east of the fault on the south wall of trench BMT–1, the unit appears to be unfaulted; its thickening appears to be due to typical downslope colluviation across the fault scarp.

Units II and III (pl. 20) form a single continuous soil profile; therefore, they were deposited long before the faulting event that displaced them, on the basis of the well-developed soil horizon preserved on the hanging wall near the fault. Unit III has been eroded from the footwall and is present only east of the fault, where the unit has been backtilted. We believe that the apparent thickening of unit III, where it overlies the fissure fill of unit II debris adjacent to the fault (sta. 18 m), resulted from the erosion of unit III deposits from the footwall and subsequent deposition after the faulting event. Thus, unit III, as mapped near the fault, probably includes some postfaulting, scarp-derived colluvium (reworked unit III). A separate colluvial-wedge unit could not be distinguished, possibly because of masking by subsequent pedogenesis. Backtilting and fissure filling similar to that observed in the south wall (stas. 17–19 m) are commonly observed in trench exposures across Quaternary normal faults and are features associated with historical surface-rupturing normal-faulting earthquakes in the Basin and Range Province (Nelson, 1992; McCalpin and others, 1994). The fissure fill that is composed solely of unit II material overlain by overthickened unit III deposits indicates only one faulting event since the deposition of units II and III. In addition, no buried soil horizons, stonelines, or texturally different fissure fills are present that would indicate multiple displacements of units II and III. Therefore, we interpret the above observations to indicate that the Tarantula Canyon trench site (fig. 47) has undergone only one faulting event since the deposition of those units.

Numerous fractures are present in the hanging wall in unit II (stas. 3–18 m, south wall, pl. 20). Though not recognizable in unit III, possibly either because they healed during subsequent pedogenesis or because they were never well developed in the clayey material of that unit, the fractures are believed to have resulted from the faulting event that offset and backtilted both units II and III and created the scarp. Stratigraphic relations of the carbonate laminae filling some fractures in unit II also indicate that this unit may have been fractured not only during the 1.5-m-displacement faulting event but also during a later faulting event. If such faulting events occurred, no measurable displacement was observed. We conclude that if a paleoearthquake other than the 1.5-m-displacement faulting event occurred on the Bare Mountain Fault at Tarantula Canyon (TC, figs. 46, 47) and produced some of the fractures in unit II, its magnitude was below the threshold of surface rupture, which in the Basin and Range Province is believed to be about M_W=6.5 (dePolo, 1994).

Backtilting of unit II on the hanging wall is particularly pronounced between stations 16 and 18 m but is present in the trench eastward to at least station 5 m (south wall, pl. 20). To compensate for the backtilting, vertical separation resulting from the faulting event was measured by projecting the nearly flat surface of the calcic soil horizon from both ends of the trench into the fault. Total vertical separation of unit II across the fault is about 1.5 m down to the east (fault strikes N. 40° E. and dips 72° SE.). No indication of lateral or oblique slip was observed in the trench. Slickensides with near-vertical rakes on bedrock and on silica- and carbonate-cemented gravel along the fault north of Tarantula Canyon (TC, figs. 46, 47) indicate that past displacement on the fault in this area has been nearly pure dip slip.

Discussion

Unit IV is the only unfaulted deposit in trench BMT–1 (pl. 20; figs. 1, 47). Therefore, the age of this unit, which is estimated at latest Paleocene to early Holocene (6±1 ka; sample TL–31, table 38), provides a minimum date for the most recent faulting event at the Tarantula Canyon trench site. Four lines of evidence, from both the trench and the surrounding area, indicate that the date of the most recent faulting event may be much older than Holocene.

First, a distinct laminar carbonate layer, 0.5 to 1.5 cm thick, is present at the contact between units II and IV on the footwall block (stas. 18–23 m, south wall; stas. 20.5–23 m, north wall, pl. 20). This laminar carbonate layer appears to postdate the most recent faulting event because it drapes the 72°-dipping fault plane, coating cobbles and pebbles along the fault surface, and because it thins with depth, extending nearly to the bottom of the trench. The carbonate layer retains its laminar characteristics and is not brecciated, fractured, or striated, as would be expected if it had been faulted. In addition, pieces of this laminar carbonate are absent in the fissure-fill material. The laminar carbonate is not present on either trench wall where unit II has been backtilted downward. A similar carbonate layer on unit II is in the eastern part of the trench (sta. 8 m) and alternately truncates and infills fractures in unit II. Thus, the estimated time interval required to develop the 0.5- to 1.5-cm-thick laminar carbonate layer constrains the

Table 38. Numerical ages of surficial deposits exposed in trenches BMT–1 and BMT–2 across the Bare Mountain Fault, southwestern Nevada.

[See plates 20 and 21 and figures 1, 2, 47, and 48 for locations. All samples, thermoluminescence analyses by S.A. Mahan; error limits, ±2σ]

Trench	Sample	Unit and material sampled	Estimated age (ka)
BMT–1 (pl. 20)	TL–31	IV, sediment surrounding artifact----	6±1
	TL–32	III, sand--------------------------------	16±1
BMT–2 (pl. 21)	TL–33	III, sandy-silty gravel-----------------	5.5–10

date of faulting better than the estimated age of unit IV alone. The thermoluminescence age of 16±1 ka (sample TL–32, pl. 20; table 38) on the carbonate may provide a minimum date for the most recent faulting event at Tarantula Canyon.

Second, pedogenic carbonate has overprinted unit III and is traceable across the fault zone (stas. 17–18 m, south wall, pl. 20) to the base of unit IV. The calcic soil horizon on unit III at the fault probably developed contemporaneously with the laminar carbonate layer at the top of unit II. The base of the calcic soil horizon approximately parallels the ground surface, indicating that this soil profile is unfaulted. Thus, the estimated time interval required to erode unit III, deposit unit IV, and develop $CaCO_3$ stage I+ morphology within both units III and IV also would constrain the date of faulting better than the estimated age of unit IV alone.

Third, the topographic profiles of the scarp support a date of several tens of thousands of years for the latest faulting event at Tarantula Canyon and the interpretation of only a single surface-rupturing paleoearthquake since the deposition of units II and III. As discussed above, the profile data indicate that the scarp at this site significantly predates the Beatty scarp (9–13 ka) and could be dated at near 100 ka. Also, no bevels or compound scarps are discernible in the scarp profiles. Furthermore, the surface offset (1.5 m) measured from the profile (3, table 37) at the trench site is consistent with the vertical separation (1.5 m) of unit II measured in the trench. These observations indicate only that one faulting event has occurred at the site and that it was relatively old.

Finally, the small debris-flow deposit (unit Q3?, fig. 47) mapped north of Tarantula Canyon Wash (TCW, fig. 46) postdates the latest faulting event. This deposit originated from a side drainage and buried unit Q2 alluvium. No fault scarp is present on the unit Q3? surface, as indicated by a topographic profile (9, fig. 47) that extends across the projection of the scarp. The debris-flow deposit that buries the fault has a well-developed argillic soil horizon with $CaCO_3$ stage II+ morphology; this deposit apparently accumulated before most of the downcutting along Tarantula Canyon Wash. Both of these pieces of evidence from the north side of Tarantula Canyon Wash support a date of at least several tens of thousands of years for the most recent surface rupture in the area.

Wildcat Peak Trench Site

The Wildcat Peak trench site (pl. 21; figs. 46, 48) is located at the Bare Mountain range front, east of a prominent peak of the same name. The site was selected for detailed study because, in a mining-exploration pit located at the fault zone, Reheis (1988) reported evidence indicative of late Pleistocene and, possibly, Holocene displacement. The pit does not cross, nor is it associated with, an obvious fault scarp on a Quaternary alluvial-fan surface.

Near the mining-exploration pit, which is identified in the present report as trench BMT–2 (figs. 1, 48), the range front is marked by an abrupt linear, N. 25° E.-trending contact between Paleozoic bedrock and Quaternary alluvial-fan deposits (primarily unit Q4, table 35). About 240 m northeast of the trench, the linear range front is on trend with a bedrock fault mapped by Monsen and others (1992); however, no features in Quaternary deposits interpreted to be fault scarps have been identified in this area.

Unit Q4 alluvial-fan deposits (latest Pleistocene to Holocene) are the most common along the range front at the Wildcat Peak trench site (pl. 21). Several small remnants of unit Q3 deposits also have been identified (fig. 48). At one locality, approximately 600 m north of trench BMT–2, a unit Q3 alluvial fan that crosses the range front is preserved. No scarp is present on the unit Q3 alluvial-fan surface, indicating that it postdates any surface rupture along the Bare Mountain Fault at this locality. At another locality about 100 m south of trench BMT–2, an arcuate, 50-m-long scarplike feature that is particularly prominent under low-sun-angle conditions was identified by Monsen and others (1992) as a fault displacing older alluvial-fan deposits. We interpret this scarplike feature, however, to be the frontal lobe of a small debris flow (unit Q4d, fig. 48) that postdates unit Q3 alluvium exposed farther east, on the basis of its more pronounced bar-and-swale morphology and a thinner Av soil horizon than are typical of the older unit.

Stratigraphy

Trench BMT–2 (pl. 21; figs. 1, 48) is located on an alluvial-fan complex of unit Q4 (table 35) age and between small active channels of unit Q5 age (fig. 48; active channels not shown). Four major alluvial and colluvial deposits, two possible fissure-fill units, and bedrock are exposed in the trench. Dolomite of Cambrian age forms the footwall; in the north wall it is highly resistant, though brecciated and fractured, and in the south wall it is hydrothermally altered (red versus unaltered grayish black), brecciated, and highly sheared. In the north wall, below the level of the former ground surface, the resistant bedrock is covered by a thick silica and carbonate coating. The silica and carbonate extend down to 3-m depth and form vertically orientated slabs, some with striations and grooves, between the alluvium and bedrock.

The four alluvial and colluvial deposits exposed in trench BMT–2 were derived from two different sources, as indicated by differences in the relative abundance of clasts from two of the Cambrian formations (Zabriskie Quartzite and Bonanza King Formation; see Monson and others, 1992) exposed nearby. Thus, correlation and differentiation of the units exposed in the two trench walls are difficult. Unit I, consisting of massive, sandy-bouldery gravel, is the lowermost and oldest unconsolidated deposit recognized in both walls of trench BMT–2. The unit consists of clast-supported gravel containing angular to subangular cobble- to boulder-size clasts, some as large as 75 cm in diameter. A unique characteristic is that, although the unit is immediately adjacent to dolomite of the Bonanza King Formation that forms the footwall, as much as 95 volume percent of the clasts in the unit are of Zabriskie Quartzite. A silica-carbonate soil horizon (Bk, $CaCO_3$ stage II+–III morphology; soil-profile description BMT–2S), from a few centimeters to nearly 50 cm thick, is present in the upper part of the unit (C, south wall, pl. 21). The silica-carbonate soil horizon associated with unit I overlies and either truncates or completely masks the shears and faults within unit I. On the north wall, a distinct stoneline consisting of clasts with thick silica and carbonate rinds and pendants is present at the top of unit I. Unit IC, a colluvial deposit that is present only on the north wall of trench BMT–2, is a sandy-cobbly gravel, as much as 30 cm thick. The unit also is characterized by thick silica and carbonate coatings and pendants on clasts and is differentiated from unit I by a distinct stoneline between the two units. Although the age of unit I is unknown, the moderate silica and carbonate cementation ($CaCO_3$ stage II+ morphology) indicates some antiquity, probably tens of thousands of years.

Unit II (pl. 21) consists of massive silty-sandy gravel, 20 to 70 cm thick, that has a distinctive erosional contact with the underlying unit I. Unit II is present only on the south wall of the trench and may be correlative with either unit IC or III on the north wall.

On the north wall, unit III (pl. 21) is a sandy-silty gravel, as much as 1 m thick. Approximately equal proportions of the clasts in this unit are of Bonanza King Formation and Zabriskie Quartzite. The unit has a moderately well developed carbonate soil horizon ($CaCO_3$ stage I+–II morphology), and individual clasts have carbonate coats and pendants. Unit III is differentiated from underlying units by its moderately well developed soil, its greater abundance of dolomite clasts, its finer texture, and the distinct stoneline at its base. The unit appears to be the equivalent of unit Q4 (table 35). Its soil-profile development indicates an age probably no older than latest Pleistocene, which is supported by a thermoluminescence age of 5.5–10 ka obtained for sample TL–33 (pl. 21, table 38).

Unit IV (pl. 21) consists of sandy-silty gravel, 15 to 40 cm thick. The unit in the south wall of the trench is composed of only 10 volume percent clasts of Bonanza King Formation, even though outcrops of this dolomite are immediately upslope. The unit has a weakly developed Av soil horizon in the upper few centimeters, as well as weak carbonate cementation ($CaCO_3$ stage I morphology). On the basis of soil-development characteristics, unit IV is dated at Holocene, possibly even late Holocene.

In addition to the above units, two possible fissure fills have been identified in trench BMT–2 (pl. 21; figs. 1, 48) on the basis of their loose texture and scattered clasts with nearly vertical long axes. In the north wall, between stations 3.5 and 6.5 m, fissure fill 1 lies within unit I. In the north wall (sta. 2.5 m), fissure fill 2 consists of a mass of loose material composed of clasts of laminar silica and carbonate, as well as quartzite. Fissure fill 2 lies between the bedrock surface and units I and III. In the south wall, fissure fill 1 is mapped between stations 7 and 8.5 m, and fissure fill 2 is immediately adjacent to the exposed bedrock. Clasts of laminar silica and carbonate are absent in fissure fill 2 in the south wall of the trench.

Interpretation of Quaternary Fault Activity

In trench BMT–2 (pl. 21; figs. 1, 48), the Bare Mountain Fault is expressed by fissure fills, altered and brecciated rock, and a bedrock fault surface that dips 62°–74° E. Because of the absence of readily correlatable units on opposite sides of the fault, the paleoseismic history of the Bare Mountain Fault at this site is difficult to decipher. The location of the trench, immediately adjacent to a bedrock outcrop, also results in very coarse grained deposits, in turn, making it difficult to identify fractures and faults and to differentiate stratigraphic units. However, evidence for at least two faulting events is apparent.

The first faulting event produced the fractures present in several places in unit I (pl. 21). This faulting event(s) also resulted in the formation of the large fissure fill (1, pl. 21) visible in both trench walls, identified by its loose texture and subvertical to vertical clast orientation. Clasts in the adjacent indurated unit I deposits are nearly horizontal. In the south wall of the trench, fissure fill 1 and individual shears or fractures east of station 8.5 m are clearly overprinted by the overlying Bk soil horizon (C, pl. 21); on the north wall, the fissure fill and associated fractures are overlain by unit IC. The amount of stratigraphic separation associated with this event(s) is not measurable in this trench.

A second faulting event appears to displace unit I and fissure fill 1 along the bedrock fault surface (stas. 8.5–9.5 m, south wall, pl. 21). Unit II partly infills the fault zone, but the unit II surface parallels the present ground surface and thus postdates the most recent faulting event. In addition, unit II is not fractured and shows no evidence of shearing. The distance from the top of unit I on the hanging wall to the top of bedrock on the footwall indicates that the displacement associated with this faulting event could be about 1 m; however, without correlative units on opposite sides of the fault, the exact displacement is not accurately measurable. As expressed in the north wall of the trench, the most recent faulting event apparently produced the loose zone (fissure fill 2) containing clasts of laminar silica and carbonate. Reheis (1988) suggested that the clasts in this loose zone could be faulted pieces of a laminar carbonate horizon, 1 to 2 cm thick, at the top of our unit I. However, the massiveness and laminarity of the silica and carbonate clasts in fissure fill 2 (typically 5–10 cm thick) indicate that the clasts are not from unit I. We interpret these clasts to be part of unit QTa (table 35) or a similar deposit. In the north wall, the unit we infer to be fissure fill 2 rests directly on the bedrock fault surface in the middle and lower parts of the trench, but what appears to be an upward extension of the fissure fill separates a small colluvial wedge (unit III?) next to the fault from the main part of unit III to the east. The implication of these relations, with regard to whether unit III is faulted, is discussed in the next subsection.

Unit IV is clearly unfaulted in trench BMT–2 (pl. 21; figs. 1, 48). Therefore, its age, probably no older than middle Holocene, provides a minimum date for the most recent faulting event at the Wildcat Peak trench site.

Discussion

Interpretation of the Quaternary activity on the Bare Mountain fault, as expressed in trench BMT–2 (pl. 21: figs. 1, 48), is difficult. Reheis (1988) concluded that evidence for two faulting events was present in the north wall of the trench. We agree with her conclusion but differ on interpretation of the dates for the two faulting events, partly because our interpretation relies substantially on geologic relations that either are observed on the surface in the area surrounding trench BMT–2 or are exposed in trenches BMT–1 (pl. 20) and BMT–3 (pl. 22), which were unavailable for Reheis' study.

The origin and date of deposition of at least the upper part of the loose zone of silica and carbonate rubble (fissure fill 2, pl. 21) between units III and III? on the north wall of the trench are uncertain. The deposit could be interpreted to indicate that units III and III? are faulted; however, evidence from the south wall of the trench and geologic relations observed north and south of the trench do not support such an interpretation. Similar to the interpretation from trench BMT–1 (pl. 20), the estimated age for the only exposed unit that is clearly unfaulted (unit IV, possibly late Holocene), provides a minimum date for the most recent surface rupture on the Bare Mountain Fault at the Wildcat Peak trench site (fig. 48). Two lines of evidence, however, indicate that the surface rupture there is probably no younger than latest Pleistocene.

First, in the south wall of trench BMT–2 (pl. 21), unit II overlies sheared fissure fill 2 at the bedrock-alluvium contact and appears to be unfaulted. Soil development on unit II displays $CaCO_3$ stage II morphology, indicating a pre-Holocene age.

Second, the surficial geology at the Wildcat Peak site (fig. 48) shows no evidence of scarps on upper Pleistocene deposits (unit Q3, table 35) north and south of the site. As discussed above, a unit Q3 alluvial fan (estimated to be late Pleistocene), 600 m north of trench BMT–2 (pl. 21; figs. 1, 48), is unfaulted, and unit Q4 alluvial fans (latest Pleistocene to Holocene) north and south of trench BMT–2 are unfaulted as well. If a Holocene faulting event occurred, all of these fans should show some evidence of faulting or fracturing in the form of vegetation lineaments, tonal contrasts, or topographic scarps.

Our initial conclusion regarding the faulting history at trench BMT–2 is that evidence exists for two faulting events during middle to late Pleistocene time. However, the most recent faulting event probably was no later than late Pleistocene. Although the amount of displacement associated with faulting events at this study site is difficult to determine, the recurrence interval for faulting events appears to be long, on the basis of the soil horizon ($CaCO_3$ stage II+ morphology) developed on unit IC. This unit clearly postdates the penultimate faulting event but predates the most recent faulting event. The carbonate cementation in unit II on the south wall also indicates that a considerable time interval elapsed between the two faulting events at the trench site, an interpretation consistent with observations at the other trench sites (BMT–1, BMT–3).

Stirling Trench Site

The Stirling trench site (pl. 22; fig. 49), located near the south end of Bare Mountain about 1.5 km north of Steves Pass (fig. 46), was selected for detailed study because it is the only trench site toward the south end of the Bare Mountain Fault with a well-defined scarp on a middle Pleistocene alluvial-fan surface (unit Q2, table 35). The site is abreast of extensive outcrops of the Stirling Quartzite of Late Proterozoic age (Monson and others, 1992), which is the source for the monolithologic alluvial fans in the area. The range front at the Stirling trench site is relatively low, with only about 200 m of relief, indicating that the displacement of bedrock on the fault is less there than near Tarantula Canyon, where the topographic relief approaches 700 m.

The scarp in Quaternary deposits at the Stirling trench site is slightly arcuate, trends nearly north-south to about N. 40° W., and is approximately 250 m long (fig. 49) and 1 to 3 m high. The scarp is present on remnants that are interpreted to be part of a unit Q2 (table 35) alluvial fan (middle Pleistocene). The alluvial-fan deposits appear to be relatively thin, partly overlying bedrock of the Wood Canyon Formation (Monsen and others, 1992) of Early Cambrian and Late Proterozoic age. The unit Q2 alluvial-fan surface is fairly steep (average slope, 8°–11°), with a subdued bar-and-swale topography and a moderately well developed desert pavement. Boulders and cobbles on the alluvial-fan surface are of light-gray to white quartzite, derived from outcrops of the Stirling Quartzite upslope to the west (Monsen and others, 1992). Many of the quartzite clasts have moderately dark to dark rock varnish, and many clast bottoms are reddened. The middle Pleistocene age for the unit Q2 alluvial fan is based on collective surface characteristics (table 35) and the stratigraphic position of the alluvial fan relative to surrounding fans. No scarps have been identified on units Q3 and Q4 alluvial fans to the north and south of the scarp at the Stirling trench site.

Scarp Profiles

Six topographic profiles were measured at the Stirling trench site (pl. 22; fig. 49). Maximum scarp slopes range from 14° to 20°, and maximum scarp heights from 1.2 to 3.3 m (table 37). In figure 50, data for the Stirling scarp are plotted against data for the dated Beatty scarp (9–13 ka), the regressions of Bucknam and Anderson (1979), and the data for the Tarantula Canyon scarp. Scarp heights for the Stirling and Tarantula Canyon scarps are similar, but maximum slopes for the Stirling scarp are steeper than those for the Tarantula Canyon scarp and more comparable to those for the Beatty scarp. Although the Stirling scarp is younger (see fig. 50) and so has been subjected to a shorter period of degradation, we believe that the higher slope angles at that trench site result primarily from the steeper slope of the alluvial-fan surface there than at the Tarantula Canyon trench site (5°–11° versus 1°–3°).

Stratigraphy

Trench BMT–3 (pl. 22; figs. 1, 49), a 26-m-long excavation, exposes at least eight major lithologic units and (or) soil horizons. All the surficial deposits are of alluvial, colluvial, or eolian origin, and all the contained clasts are of Stirling Quartzite. Sheared and altered quartzite, believed to be in the Wood Canyon Formation, forms the oldest unit exposed in trench BMT–3; the unit is present only in the footwall. The upper 40 to 60 cm of the quartzite is strongly impregnated with carbonate.

Overlying the altered quartzite and known to be present only on the footwall is a carbonate-cemented sandy gravel (unit I, pl. 22). As exposed, the unit consists of a soil horizon with well-developed $CaCO_3$ stage IV morphology. Cementation is so strong that, when excavated, clasts of Stirling Quartzite break as readily as the carbonate cement. Unit I, which is typically 10 to 60 cm thick, appears to form a pediment gravel on the underlying Wood Canyon Formation. The strong carbonate cementation may have been enhanced by the shallow depth to bedrock below unit I, with the less permeable bedrock hindering infiltration to some extent. This soil development may also reflect some antiquity; however, because unit I remained near the ground surface on the footwall while deposits on the hanging wall were being buried, the carbonate soil horizon developed on unit I could be equivalent to one or more of the three carbonate soil horizons developed on units in the hanging wall.

Unit II, at the base of trench BMT–3 (pl. 22; figs. 1, 49) on the hanging wall, consists of poorly stratified sandy gravel, more than 50 cm thick. The unit, which has stage $CaCO_3$ I+–II morphology, is interpreted to be the Bk soil horizon associated with the A and Bt soil horizons preserved in the overlying unit V. Unit II? is a small wedge-shaped deposit, about 80 cm thick, consisting of carbonate-cemented, clast-supported, angular to subangular pebbles and cobbles in a sandy matrix on the footwall block. The deposit lies unconformably on both unit I and altered bedrock of the Wood Canyon Formation. Units II and II? are believed to be correlative on the basis of their stratigraphic position, apparent thicknesses, and similar sedimentologic characteristics. Although the carbonate development is more advanced in unit II? than in unit II, the difference is considered to be the result of one unit (II?) being at shallower depth on the footwall and the other unit (II) being more deeply buried on the hanging wall.

Unit III (pl. 20) consists of poorly stratified, sandy to clayey gravel, 40 to 60 cm thick, that is interpreted to be the A-Bt horizons of a buried soil (with unit II as the associated carbonate horizon). The unit is present only on the hanging-wall side of the fault and is distinguishable from overlying and underlying units by its generally smaller clast size and matrix-supported texture. The upper 25 cm is interpreted to be a buried A soil horizon because of its color, texture, and relation to the Bt soil horizon in the lower 20 to 50 cm. The unit has $CaCO_3$ stage II morphology, which may be partly inherited from overlying unit V. Units II and III on the hanging wall clearly are not correlative with units I and V on the footwall, on the basis of thickness and sedimentologic characteristics. Units II, II?, and III appear to form a single depositional package, partly because unit II? on the footwall clearly truncates unit I and because it underlies and is truncated by unit V.

Unit IV (pl. 22) consists of carbonate-cemented sandy gravel, typically 50 to 70 cm thick. Pebbles and cobbles are generally clast supported and exhibit subhorizontal fabric. The unit, which has $CaCO_3$ stage II+–III+ morphology, including incipient $CaCO_3$ stage IV morphology in its upper part (laminae several millimeters thick in places), is interpreted to be the calcic (Bk) soil horizon associated with overlying soil horizons in units V and VI. The strong carbonate cementation in unit IV appears to be similar to that in unit II?, indicating that both units represent the same period of soil formation, although they do not correlate depositionally or stratigraphically.

Unit V (pl. 22), on the footwall, consists of clayey gravel, generally 45 to 70 cm thick. The unit exhibits angular-blocky soil structure and clay films that are readily visible without magnification, with a strongly developed argillic (Bt) soil horizon that may partly be associated with the strong carbonate developed in unit I. However, although the contact between unit V and the underlying unit I is abrupt, it is also wavy and exhibits relief (10–35 cm; pl. 22). This contact indicates a hiatus marked by erosion of the top of unit I before deposition of unit V. The soil properties of unit V weaken toward the surface scarp and the associated fault zone, apparently owing to the unit's position on the steeper part of the slope. Thus, we have subdivided unit V into units V, Va, and Vb on the basis of soil development. Both units Va and Vb, though slightly weaker, retain argillic soil-horizon characteristics similar to those of the rest of unit V. On the basis of stratigraphic position, texture, and soil development, unit V on the footwall is correlated with unit V in the hanging wall.

Unit V (pl. 22), on the hanging wall, consists of angular clasts of Stirling Quartzite in a clayey, silty, and sandy matrix. The unit, which is 50 to 120 cm thick, displays strong prismatic structure; distinct clay films are visible without magnification. Unit V is interpreted to be the argillic (Bt) soil horizon associated with an overlying A soil horizon (unit VII) and an underlying carbonate soil horizon (unit IV). The upper part of unit V has $CaCO_3$ stage I+ to weak stage II morphology that appears to have been overprinted on the unit after deposition of unit VI. Unit V, along with units IV and VI, composes unit Q2 (fig. 49; table 35). Soil development on these units is consistent with the middle Pleistocene age estimated for unit Q2 (table 36).

Unit VI (pl. 22), a colluvial deposit composed of about 10 volume percent subangular pebbles and cobbles of Stirling Quartzite in a silty and sandy matrix, is continuous along the entire length of the trench but is generally much thicker on the hanging wall (30–50 cm thick) than on the footwall (10–20 cm thick; similar to unit IV in trench BMT–1, pl. 20). The unit, which is primarily the vesicular (Av) soil horizon associated with the alluvial-fan surface, includes a large eolian component. Unit VI, which also is partly composed of colluvium, loses much of its vesicularity as it crosses the scarp (stas. 10–16 m, south wall, pl. 22). The upper part of the unit displays a platy soil structure that imparts a laminar appearance.

Unit VII (pl. 22) consists of fine sand, 0 to 12 cm thick, that is probably eolian in origin. The unit forms a vesicular A (Av) horizon and is differentiated from unit VI on the basis of color, texture, and pedogenic structure. Unit VII was not differentiated on the south wall of the trench because of disturbance by excavating equipment. Its lower contact is marked by a weak stoneline that apparently represents the buried pavement of the underlying unit VI.

Two fissure fills, 1 and 2, in trench BMT–3 (stas. 11–14 m, pl. 22) are characterized by randomly oriented clasts and are uncemented to weakly cemented; fissure fill 2 is generally less strongly cemented than fissure fill 1.

At present, numerical ages have not been determined for any of the units in trench BMT–3 (pl. 22, figs. 1, 49); however, ages can be estimated on the basis of soil development, stratigraphic position, and correlations with dated units in other Bare Mountain trenches and elsewhere in the region. Unit VII is dated at Holocene (possibly late Holocene) because of its stratigraphic position and its absence of soil development. Units IV through VI appear to be a single depositional package on the basis of sedimentologic characteristics, stratigraphic relations, and soil development. Unit VI appears to be the Av soil horizon associated with units II? and V on the footwall and with units IV and V on the hanging wall. Unit V is a strongly developed Bt soil horizon, and units II? and IV are strongly developed Bk soil horizons. These three units are considered to represent unit Q2 (tables 35, 36), which likely correlates with the Early Black Cone alluvium of Peterson and others (1995). The minimum age of the Early Black Cone surface is estimated at 159–201 ka (table 36). Thus, the time interval represented by the depositional package and associated soils that compose units IV through VI is probably no younger than 159 ka.

Estimated ages for units I, II, II? and III are speculative; however, several properties indicate that they all are older than late Pleistocene. All four units are buried by unit Q2 (table 35). In addition, unit III has a well-developed argillic (Bt) soil horizon, and unit II is the associated carbonate soil horizon. Both units II and III are buried by units IV through VI and so have been below the soil-forming zone since at least 159 ka. Although the Bt soil horizon on unit III is not as well developed as on unit V, the time interval represented by the development of the Bt soil horizon in unit III probably extends at least several tens of thousands of years. Finally, unit I has a well-developed carbonate soil horizon. Unlike units II and III on the hanging wall, unit I has remained in the maximum carbonate-soil-forming zone, and so the strength of the carbonate soil horizon in unit I may represent much or all of the total time elapsed since deposition of the unit. These factors indicate that units I, II, and III are probably much older (200–500 ka) than unit Q2 (minimum estimated age, 159 ka) and its correlative units exposed in trench BMT–3.

Interpretation of Quaternary Fault Activity

Stratigraphic and structural relations exposed in trench BMT–3 (pl. 22; figs. 1, 49) indicate that at least two surface-rupturing paleoearthquakes have occurred on the Bare Mountain Fault at this site since the mid-Quaternary to late Quaternary. An obvious fault zone is exposed in the south wall of the trench (stas. 12–14 m), and the Wood Canyon Formation and Quaternary units II through V are all clearly faulted. The fault dips 79° E. Although unit VI thickens near the fault, it overlies the fault zone with no obvious displacement. However, because unit VI is interpreted to be the Av soil horizon associated with the underlying Bt and Bk soil horizons (units IV and V on the hanging wall and units II? and V on the footwall), the base of unit VI may have been offset by the most recent surface rupture. The absence of clear evidence for faulting and the thickening of unit VI across the scarp may reflect the time-transgressiveness of the unit, subsequent pedogenesis, and the relative mobility of the fine material on the alluvial-fan surface.

The sequence of events recorded by the strata exposed in trench BMT–3 (pl. 22; figs. 1, 49) is interpreted as follows: (1) erosion or pedimentation of the Wood Canyon Formation and subsequent deposition of unit I; (2) displacement of unit I by a possible faulting event(s), although no direct evidence was observed because deposits possibly correlative with unit I are not exposed on the hanging wall; (3) deposition of units II, II?, and III across the fault; (4) a period of landscape stability and development of the Bt soil horizon now preserved in unit III on the hanging wall (a correlative unit was apparently eroded off the footwall before unit V was deposited); (5) displacement of units II, II?, and III by faulting (referred to as event Y); (6) deposition of fissure fill 1 by erosion of units II, II?, and III; (7) deposition of units IV through VI across the fault; (8) a period of landscape stability and development of the Bt soil horizon on unit V and the Bk soil horizon on units II? and IV; (9) displacement of units IV through VI by faulting (referred to as event Z); (10) deposition of fissure fill 2 and thickening of unit VI in the hanging wall by erosion of material off the hanging wall; and (11) deposition of unit VII across the fault and development of the carbonate soil horizon ($CaCO_3$ stage I+–II morphology) on unit V on the hanging wall, on fissure fill 2 at the fault, and on unit V on the footwall.

The displacement associated with event Y is difficult to measure but was probably about 1.5 m. Unit III (pl. 22) appears to be backtilted toward the fault, resulting in an apparent vertical displacement of nearly 3 m if the top of that unit is projected toward the estimated position of the former ground surface. This interpretation assumes that a Bt soil horizon similar in thickness to the Bt soil horizon developed on unit III on the hanging wall was originally present above unit I on the footwall. However, if we assume that unit III had a slope similar to that of unit V and the present ground surface (approx 8°–11°), and if unit III is restored to that position, then the net slip resulting from event Y is about 1.5 m.

Measurements indicate a net slip for event Z of about 0.8 m and an apparent vertical displacement of about 0.7 m, both values determined by projecting the unit V (pl. 22) surface toward the fault zone from points about 7 m from the zone on both the hanging wall and the footwall, and by assuming a prefaulting surface slope of 11°. This slope was used because, at the trench, a scarp profile shows a relatively constant far-field slope of 11° for the unit Q2 alluvial-fan surface. These projections were also made to account for the backtilting of unit V and the apparent erosion of that unit on the footwall near the fault. Both the net slip and apparent vertical displacement agree with the surface offset of 0.8 m measured from the scarp profile (15, table 37).

Discussion

Clear evidence for at least two faulting events is preserved in trench BMT–3 (pl. 22; figs. 1, 49). The displacement associated with the latest event (Z) appears to have been about 0.8 m, but the date of this event is not well constrained. The only clearly unfaulted unit in trench BMT–3 is unit VII (Holocene). As described for trenches BMT–1 (pl. 20) and BMT–2 (pl. 21), however, the age and sedimentologic characteristics of the surficial deposits do not appear to provide an accurate estimate of the date of the most recent faulting event. A more realistic minimum date for this event can be estimated from the degree of carbonate accumulation ($CaCO_3$ stage I+–II morphology) that has subsequently overprinted unit V and fissure fill 2. On the basis of thermoluminescence analysis of a unit with similar carbonate morphology at the Tarantula Canyon trench site (pl. 20; fig. 47), we infer that the most recent event at the Stirling trench site (pl. 22; fig. 49) probably occurred before 16±1 ka (sample TL–32, table 38).

Additional geologic relations at the Stirling trench site (pl. 22; fig. 52) also support the interpretation that the most recent faulting event there is at least latest Pleistocene. No scarps are present on unit Q4 (latest Pleistocene to Holocene) and unit Q3 (late Pleistocene) alluvial fans immediately north and south of the trench site. Correlation of the unit Q3 alluvial fans to the Late Black Cone surface of Peterson and others (1995) indicates that the Q3 alluvial fans near the Stirling trench site are at least 17 ka, possibly older than 30 ka; the latest faulting event (Z) would therefore be still older. The characteristics of the fault scarp at the Stirling trench site, which are similar to those of the fault scarp at the Tarantula Canyon trench site (pl. 20; fig. 47), also indicate that the most recent faulting event at the Stirling site is no younger than late Pleistocene and could be much older.

The number of earlier faulting events, their age, and their associated displacements can only be estimated. Bt soil-horizon development on units III and V (pl. 22) and carbonate-soil development on units I, II?, and IV provide evidence that a considerable time interval is represented by the strata exposed in trench BMT–3 (pl. 22, figs. 1, 49). Stratigraphic relations indicate that these units have been offset at least twice, and the soil development on units IV and V on the hanging wall and on units II? and V on the footwall support a conclusion that a considerable time interval (possibly as much as 100–200 k.y.) elapsed between the most recent faulting event (Z) and the penultimate faulting event (Y). Thus, event Y probably occurred several hundred thousand years ago. The degree of soil development on units II and III (soils preserved only on the hanging wall) also indicates a lengthy period of time (several tens of thousands to hundreds of thousands of years) between event Y and any earlier faulting event(s).

As discussed earlier, the net slip from penultimate event Y is estimated at 1.5 m. The displacement could conceivably be as much as 3 m (top of unit III to top of unit II? minus 0.8 m for the latest faulting event); however, by restoring the slope of unit IV to about 11°, which is the present slope of the unit Q2 (tables 35, 36) alluvial fan, we obtained the estimate of 1.5 m. This value is approximately double the estimated displacement from event Z (0.8 m), indicating either that the slips associated with faulting events at the Stirling trench site (pl. 22; fig. 49) have not been uniform or that the 1.5 m represents more than one faulting event. The first interpretation appears to be more likely because direct geologic evidence for additional faulting events is absent in the trench.

Summary of Quaternary Faulting Events

Evidence based on (1) geologic relations exposed in three trenches excavated across the Bare Mountain Fault trace along the east front of Bare Mountain; (2) the distribution, correlation, and estimated ages of Quaternary surficial deposits mapped in the vicinity of the trenches; and (3) the presence or absence of fault scarps in these deposits leads to the general conclusions that no faulting events have occurred during Holocene time and that the most recent faulting event was no later than late Pleistocene. The second conclusion is supported by observations that fault scarps indicative of Quaternary activity are present only on alluvial-fan deposits dated at middle Pleistocene (minimum estimated numerical age, 159 ka). A comparison of scarp profiles measured at the Tarantula Canyon trench site (pl. 20; fig. 47) along the Bare Mountain Fault with scarps of known ages elsewhere in the region also indicate a date possibly as early as, or earlier than, 100 ka. Younger, unfaulted alluvial-fan deposits are prevalent along the mountain front, thus also providing ample supporting evidence for the interpreted date of the most recent faulting event on the Bare Mountain Fault.

At least two Quaternary faulting events are recorded in two trenches (BMT–2, pl. 21; BMT–3, pl. 22), but only one in the third trench (BMT–1, pl. 20). The date of the most recent faulting event at all three trench sites appears to be about the same, on the basis of scarp-profile data, stratigraphic relations, fault characteristics, and soil development. Because these three sites span nearly the entire 20-km length of the Bare Mountain Fault, we conclude that this most recent faulting event ruptured nearly the entire fault rather than only local segments.

Dates of faulting events that predate the most recent event (Z) cannot be reliably estimated on the basis of data from either trench BMT–2 (pl. 21) or trench BMT–3 (pl. 22). Carbonate soil development in some of the deposits exposed in trench BMT–2 indicates that a considerable time interval elapsed between event Z and the penultimate event (Y), possibly several tens of thousands of years to several hundred thousand years. Similar lines of evidence in trench BMT–3 indicate that at least 100–200 k.y. elapsed between these two faulting events. One or more earlier faulting events may have occurred at the Stirling trench site, separated from event Y also by a long interval (several tens of thousands of years to several hundreds of thousands of years), but the evidence is inconclusive.

At the Tarantula Canyon trench site (pl. 20; fig. 47) near the north end of the Bare Mountain Fault (trench BMT–1), where we observed direct evidence for only one faulting event, the relatively flat alluvial-fan surface and the well-developed carbonate soil horizon present on unit V together provide an excellent datum for measuring single-event surface displacement or offset. After compensating for the backtilting of unit V on the hanging wall, the net tectonic displacement of this unit is 1.5 m, in good agreement with the surface offset measured from scarp profiles at the trench site. Net slip associated with the most recent faulting event (Z) at the Stirling trench site (trench BMT–3, pl. 22) is well constrained at about 0.8 m. Displacement from the penultimate faulting event (Y) is estimated at 1.5 m, but the evidence is equivocal, and this offset could represent more than one faulting event. In the context of fault displacements per event, however, we consider this 1.5-m offset to reflect event Y at the Stirling trench site. Accordingly, measured per-event displacements at the three trench sites on the Bare Mountain Fault are 0.8, 1.5, and 1.5 m, from which we infer that the typical or average displacement associated with a faulting event on the Bare Mountain Fault is probably 1.0 to 1.5 m.

Accurate measurements of displacement resulting from the most recent faulting event (Z) on the Bare Mountain Fault were made at trench BMT–1 (pl. 20; figs. 1, 47) near the north end of the fault and at trench BMT–3 (pl. 22; figs. 1, 49) near the south end. Because the measured displacements associated with historical surface-rupturing earthquakes show that displacement diminishes near the ends of faults, the displacements measured at these trench sites may not represent the maximum displacement that occurred everywhere along the

Bare Mountain Fault during this event. Although we have no specific information about the displacement near the center of the fault, our conclusion is that the per-event displacement probably averages about 1.0 to 1.5 m (see below). This value is higher than the 0.5-m displacement estimated by using the data of Wells and Coppersmith (1994) for a 20-km-long fault; however, considerable scatter exists in the limited data for displacement versus fault-rupture length on normal faults.

Recurrence Interval and Slip Rate

Even though numerical-age information is limited, the relative-age data, as noted earlier, indicate that the recurrence interval for moderate to large surface-rupturing paleoearthquakes on the Bare Mountain Fault is long, probably at least tens of thousands of years. In fact, the Bare Mountain Fault appears to be a low-activity fault similar to the Santa Rita and Horseshoe Faults in Arizona, in the southern part of the Basin and Range Province, where the recurrence interval for large earthquakes appears to range from tens of thousands of years to possibly several hundred thousand of years (Pearthree and Calvo, 1987; Piety and Anderson, 1991). Thus, the available evidence strongly indicates that the Bare Mountain Fault can best be characterized as a fault with moderate to large, but infrequent, earthquakes.

At the Tarantula Canyon trench site (pl. 20; fig. 47), a unit Q2 (tables 35, 36) alluvial fan (trench units II, V) with an estimated age of at least 159 ka is displaced 1.5 m along a 72°-dipping fault (pl. 20). On the basis of this relation, the resulting slip rate (net slip or dip slip) for the Bare Mountain Fault at this site is 0.01 mm/yr. Considering that unit Q2 is probably older than 159 ka, the actual slip rate is probably even less than 0.01 mm/yr.

At the Stirling trench site (pl. 21; fig. 48), a unit Q2 (tables 35, 36) alluvial fan is displaced only 0.8 m by the most recent faulting event along a 79°-dipping fault. However, trench BMT–3 (pl. 22; figs. 1, 49) also displays evidence for multiple events. Total calculated mid-Quaternary to late Quaternary displacement there is at least 2.3 m but could be as much as about 4 m (if backtilting is not removed). If we assume a minimum age of 200 ka for the older displaced surficial trench units (II, II?, and III) in trench BMT–3 and use the 4-m estimate for total displacement, the slip rate (net slip or dip slip) for the Bare Mountain Fault at the Stirling trench site would be as high as 0.02 mm/yr. Using a more conservative age estimate of 300–400 ka for the faulted units and a value of 2.3 m for the total displacement, the slip rate at the Stirling trench site is less than 0.01 mm/yr.

A unit Q1 deposit about 3 km north of Tarantula Canyon (TC, fig. 46) is displaced approximately 4 to 5 m. Assuming a minimum age of about 500 ka for this deposit (table 36), we estimate a vertical slip rate of about 0.01 mm/yr for the Bare Mountain Fault at this site. Although the age control on the deposit there is problematic (no trenches, test pits, or numerical ages), the similarity of the estimated slip rate to those estimated at the other two sites (Tarantula Canyon and Stirling) indicates that both the estimated age and the resulting slip rate are probably reasonable.

On the basis of data from the three trench sites, the average slip rate for the Bare Mountain Fault appears to be no higher than about 0.01 mm/yr (because the steep fault dips, vertical slip, dip slip, and net slip are all nearly identical). Thus, the slip rate does not vary appreciably from north to south. Given the apparent low rates of seismicity determined in this study, we believe that additional numerical ages on faulted deposits would probably not significantly change our estimates of either the slip rate or the recurrence interval for the Bare Mountain Fault.